EUROFUSION WPPFC-PR(16) 14864

M Wirtz et al.

Transient Heat Load Challenges for Plasma-Facing Materials during Long-Term Operation

Preprint of Paper to be submitted for publication in
22nd International Conference on Plasma Surface Interactions
in Controlled Fusion Devices (22nd PSI)

This work has been carried out within the framework of the EUROfusion Consortium and has received funding from the Euratom research and training programme 2014-2018 under grant agreement No 633053. The views and opinions expressed herein do not necessarily reflect those of the European Commission.

Transient Heat Load Challenges for Plasma-Facing Materials during Long-Term Operation

M. Wirtz[1]*, J. Linke[1], Th. Loewenhoff[1], G. Pintsuk[1], I. Uytdenhouwen[2]

[1]*Forschungszentrum Jülich GmbH, Institut für Energie- und Klimaforschung, Partner of the Trilateral Euregio Cluster (TEC), 52425 Jülich, Germany*
[2]*SCK•CEN, The Belgian Nuclear Research Centre, Boeretang 200, 2400 Mol, Belgium*

*Corresponding author e-mail: m.wirtz@fz-juelich.de

Abstract

The study summarizes the experimental results on fusion relevant pure heat load exposures of different tungsten products in the electron beam devices JUDITH 1 and 2. Thereby, besides steady state heat loading, up to 10^6 transient ELM-like pulses were applied. A detailed post-mortem analysis of the obtained results exhibits a wide and complex range of thermally induced surface modifications and damages such as roughening due to plastic deformation, cracking and melting of parts of the material surface. Furthermore, recrystallization of the material, which will take place during long term operation, will additionally deteriorate the mechanical strength of the plasma facing material. Hence recrystallization and melting/re-solidification will make the material more prone to thermal shock and fatigue damages and accelerate the evolution of damages. This combination of different types of material modifications/damages accompanied by the degradation of the mechanical properties will have a strong impact on the plasma performance and lifetime of plasma facing materials/components. The additional exposure to H and He particles as well as neutrons will lead to even more severe damage formation and faster deterioration of the plasma facing materials.

Keywords:
tungsten; edge localized mode; transient thermal loads; material degradation; high pulse numbers; recrystallisation

1 Introduction

The use of plasma facing materials (PFM) over a long period of time (years, as it is foreseen already for the first ITER divertor) implies serious lifetime challenges. Especially tungsten, which will be used in the divertor region, will be exposed to severe and complex environmental conditions. Beside steady state heat loads of up to 20 MWm-2 and transient events with power densities up to 1 GWm-2 during normal operation, the PFMs also have to withstand high H, He and, although due to geometrical reasons partially shielded, neutron fluxes. So called off-normal events such as vertical displacement events (VDEs) and plasma disruptions will deposit even higher power densities on the PFM [1-3]. Most of the current research directed towards material resilience does not consider long term effects like surface fatigue by high frequency transient thermal loads or morphology changes due to creep induced by (quasi-)stationary thermal loads. The current status and available experimental results as well as the issues that were identified but not yet tackled will be presented.
In the frame of different studies the mechanical properties of various industrially produced tungsten products were characterized and tested under fusion relevant thermal loads in the electron beam devices JUDITH 1 and 2 [4-6]. Special attention was paid to the grain orientation/microstructure as well as to the recrystallised state of the materials which will

have a significant influence on the material behaviour and its mechanical properties. In order to investigate the dependence of the damage formation on the grain structure and mechanical strength low pulse number tests on different tungsten products with different power densities and base temperatures were performed. High pulse number tests (up to 106 pulses) were applied on only one material but with different grain structures as well as in the recrystallised state in order to investigate the fatigue and long term behaviour of the material. Additionally, tensile tests at different base temperatures and grain orientation were done. The obtained results reveal how the microstructure and mechanical properties are interconnected and how this affects the thermal shock response of tungsten as PFM and what will be the possible consequences for the performance of tungsten in a tokamak like ITER or DEMO.

2 Material Properties and Experimental Conditions

Four tungsten products manufactured by Plansee SE, Austria were subject to microstructure analysis, tensile tests and low pulse number experiments in JUDITH 1. These products are ultra-high purity tungsten (W-UHP, 99.9999 wt%), tungsten-vacuum-metallising-tungsten (WVMW, 15 – 40 ppm potassium) and two tungsten tantalum alloys with 1 wt% (WTa1) and 5 wt% (WTa5) of tantalum, respectively. The materials were sintered into a rod shape, thermo-mechanically deformed in axial direction obtaining a round blank with a height of ~29 mm and a diameter of ~160 mm and subsequently stress relieved at 1000 °C. Due to axial forging the grains were heavily deformed to a disc like shape perpendicular to the forging direction as shown in Figure 1a and b.

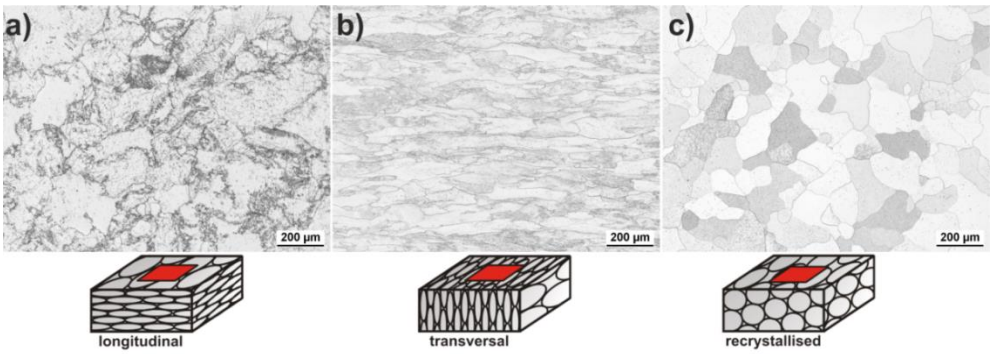

Figure 1: Light microscope images of representative examples of the deformed microstructure after the forging process: a) perpendicular to the forging direction; b) parallel to the forging direction; c) in the recrystallised state (1600 °C for 1 h).

Parts of these materials were recrystallised (see Figure 1c) according to the specifications of the supplier. W-UHP, WVMW and WTa1 were recrystallised at 1600 °C while WTa5 had to be heated to 1800 °C, because the high amount of tantalum increases the recrystallisation temperature. All four tungsten grades were kept at these temperatures for 1 h.
Based on these differences in the grain structure three different sample types for the thermal shock experiments and the tensile tests were cut for each material. Longitudinal (L) with grains oriented parallel to the loaded surface/direction, transversal (T) with a perpendicular grain orientation and in the recrystallised state (R) (schematic drawings see Figure 1). The elongation/deformation perpendicular to the forging direction is the same for all four tungsten products. After recrystallisation the anisotropy of the grains nearly disappeared. The major difference between the three tungsten grades concerning the microstructure is the grain size. W-UHP grains are more than twice as large as the grains of WVMW or WTa1 and WTa5, which have the smallest grains of the investigated materials. A possible explanation for the differences in grain size could be the addition of foreign atoms (potassium/tantalum). These represent obstacles and accordingly limit the grain growth during the manufacturing process.

However, all materials show a more homogeneous grain structure and grain growth after the thermal treatment.
Tensile tests with a deformation rate of 0.2 mm/min (deformation rate 10^{-4} s^{-1}) were performed for all four tungsten products with L, T and R microstructure (see Figure 1) at temperatures of 300 °C and 500 °C in a high temperature vacuum furnace set-up at SCK•CEN, Mol [7]. Figure 2 shows the obtained engineering stress strain curves.
Beside the expected decrease of the mechanical strength and increasing ductility at elevated temperatures for all L and R tungsten products, it can be stated that with an increasing amount of tantalum the mechanical strength of the material increases. However, this improvement of tensile strength is accompanied by a significant reduction of the total elongation. Both effects can be explained by the solid solution hardening of tungsten obtained by adding tantalum in the matrix [8,9]. W-UHP exhibits the lowest tensile strength and fracture strain, which is caused by the much higher purity and the resulting lack of foreign atoms that also causes an increase of the DBTT (ductile-to-brittle-transition-temperature) [8,10]. In contrast to the L specimens the T samples exhibit much lower mechanical strength and show brittle behaviour even at 500 °C. The reason for this anisotropic behaviour of material parameters is the so called texture strengthening effect [8,11]. For the R samples the tensile strength is the lowest of all tested materials and grain orientations. However, the total elongation is significantly higher than for the L or T grain orientation. The changes of the material parameters after recrystallisation can be explained by the thermally activated reduction of the defect density and the resulting poor cohesion between single grains, which among other material parameters increases the tensile strength [12].
The simulation of transient thermal shocks was done with the electron beam device JUDITH 1 and 2 at Forschungszentrum Jülich.

JUDITH 1
For the low pulse number thermal shock tests in JUDITH 1 12 × 12 × 5 mm³ samples were cut from all four materials with L, T and R microstructure (see Figure 1 bottom row). All samples were polished to a mirror finish to define an undamaged state. The samples were loaded with ELM relevant power densities between 0.19 GW/m² and 1.51 GW/m². These values were calculated by taking an electron absorption coefficient of 0.55 into account. A homogeneous loading of the samples was achieved by exposing a small area (4 × 4 mm²) with a focused electron beam (diameter of ~ 1 mm) at very high scanning frequencies (47 kHz in x-direction and 43 kHz in y-direction). All tests were performed with a pulse duration of 1 ms and a total number of 100 pulses. The inter-pulse time was ~ 3 s to allow a complete cool down. In addition to tests performed at room temperature (RT), a graphite holder with a tubular heating cartridge was used to achieve base temperatures up to 600 °C.

JUDITH 2
High pulse number tests were performed in the electron beam facility JUDITH 2 at Forschungszentrum Jülich. The test components consisted of tungsten tiles of 12 × 12 × 5 mm³ brazed to an actively cooled copper block. The tiles were cut from the pure tungsten grade with L, T and R grain structure and polished to mirror-like finish. The thermal shock tests were performed with power densities ranging from 0.14 to 0.55 GW/m^2, a pulse duration 0.48 ms, pulse numbers between 10^3–10^6 (loading frequency 25 Hz) and a SSHL (steady state heat load) of 10 MW/m^2. As the cooling circuit is operated with 100 °C hot water and the transient pulses also heat up the sample, the resulting surface temperature (T_{surf}) immediately before the next transient pulse is 700 °C. All tests with >10^4 pulses were interrupted every 10^4 pulses (i.e. after 400 s) for 20 s, allowing the component to return to its initial temperature (100 °C) and resembling a single ITER discharge.

After the exposure in JUDITH 1 and 2 the induced damages were investigated by SEM and laser profilometry. Subsequently, the cross sections of the samples were investigated by metallographic means to analyse the crack propagation into the bulk material.

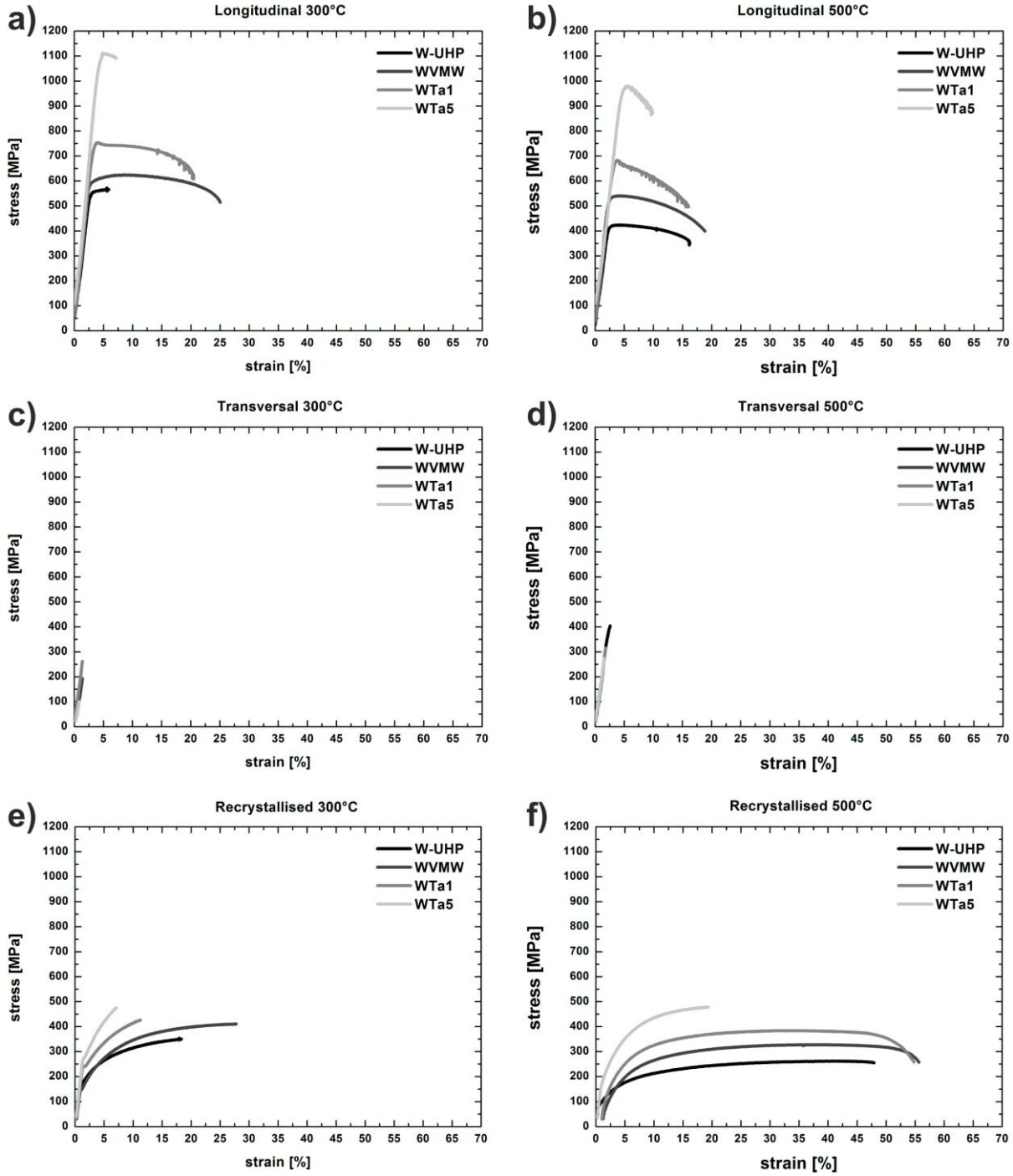

Figure 2: Engineering stress-strain diagrams of W-UHP, WVMW, WTa1 and WTa5 with longitudinal (a+b) and transversal (c+d) grain orientation as well as in the recrystallised state (e+f) with a deformation speed of 0.2 mm/min at 300 °C and 500 °C.

3 Results and Discussion

Low pulse number tests – JUDITH 1

Low pulse number tests (100 pulses) in JUDITH 1 were performed to compare the thermal shock behaviour of four different tungsten products in order to investigate which material

parameters (mechanical strength, ductility, and microstructure) influence the damage response of tungsten. The obtained surface modifications and damages for all four materials with L grain orientation are depicted in Figure 1. In these so called damage mappings the induced surface modifications and damages are colour and shape coded. This way of presentation allows defining damage (no visible damage formation below this power density) and cracking (no crack formation at higher base temperatures) thresholds for each material valid for 100 thermal shock events.

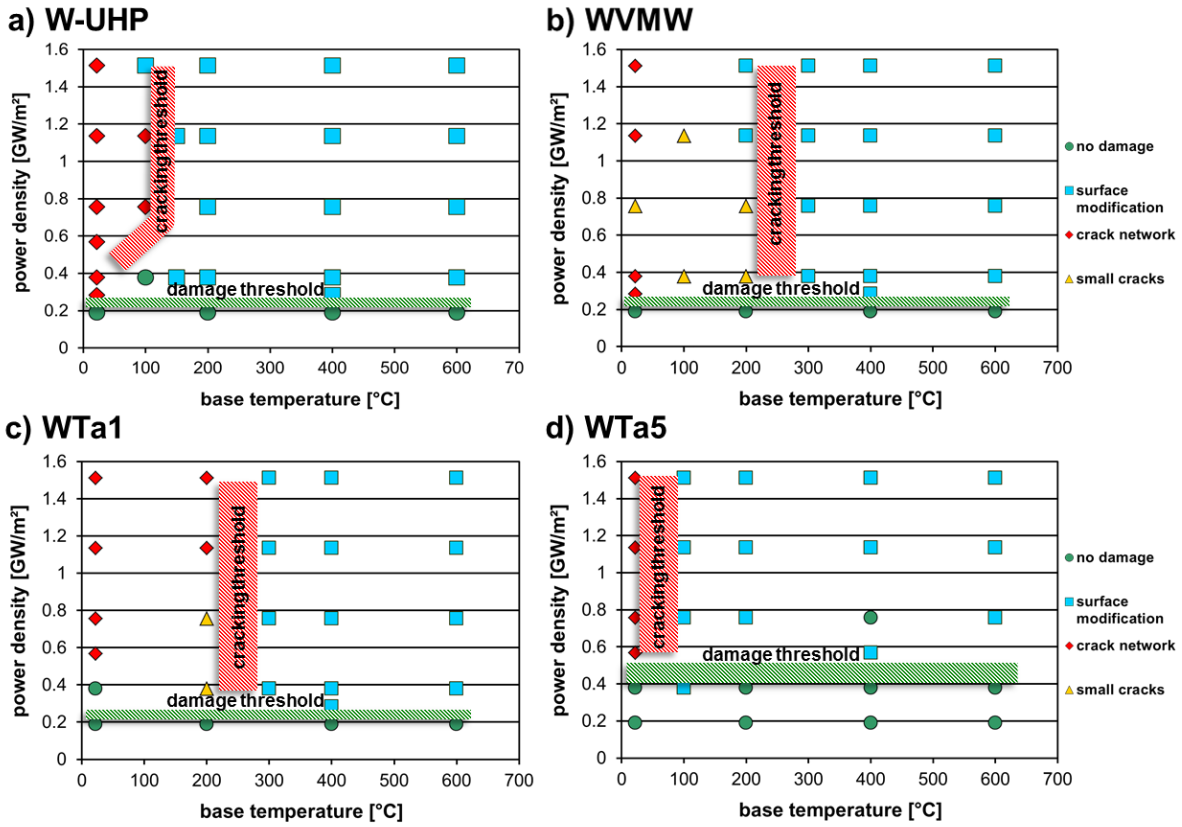

Figure 3: Thermal shock damage mappings for (a) W-UHP, (b) WVMW, (c) WTa1 and (d) WTa5 with longitudinal grain orientation [13].

The comparison of the four different materials/damage mapping shows that there are significant differences in the damage response. One of the most interesting results is the location of the damage and cracking threshold of WTa5 L. The damage threshold is located between 0.4 GW/m² and 0.6 GW/m² and hence roughly double as high as for the other three materials for which the damage is located at about 0.2 GW/m². Furthermore the cracking threshold is located at much lower temperatures (between RT and 100 °C) compared to the other materials where it varies between 100 °C and 150 °C for W-UHP L and 200 °C and 300 °C for WVMW L and WTa1 L, respectively. An explanation for this can be found in Figure 2a and b. The engineering stress-strain curves show clearly that WTa5 L has a nearly double as high mechanical strength due to the solid solution hardening by tantalum as the other materials. For example, the yield strength of WTa5 L at 500 °C is 931 MPa while the yield strength for W-UHP l and WVMW L is 408 MPa and 513 MPa, respectively. WTa1 L has a value of 652 MPa which is also higher than for W-UHP L and WVMW L but due to the lower tantalum content not high enough to have a significant influence on the location of the threshold values. Admittedly, the fracture strain of WTa 5 is with 6 % more than three times lower and due to the high content of foreign atoms not as ductile as the other materials but the

significant increase of the mechanical strength seems to compensate this at least for low pulse numbers.
Based on the damage mappings for the L orientation (see Figure 3), a reasonably reduced amount of test parameters located around the damage threshold was chosen because of the limited amount of samples/material. Figure 4 shows damage mappings for WTa5 T and R, which are here chosen as an example for the damage behaviour of these grain orientations and because of its improved damage behaviour for the L orientation.

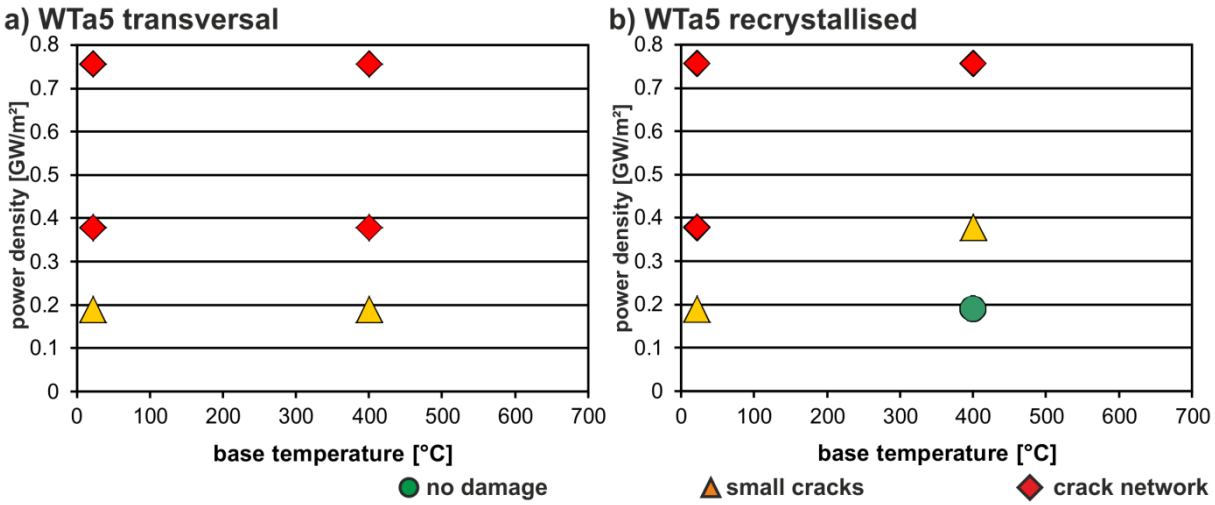

Figure 4: Damage mapping of WTa5 with (a) transversal grain orientation and (b) in the recrystallised state.

Both grain structures, T as well as R, show a severe degradation of the thermal shock performance. The damage threshold drops below 0.19 GW/m² (heat flux factor $F_{HF} \approx 6\ MW/m^2s^{0.5}$) and the cracking threshold increase to base temperatures above 400 °C. This degradation is caused by the significant drop of the mechanical strength for the T and R samples (roughly by a factor of two) as well as the brittle behaviour of T even at 500 °C (see Figure 2c and d). As a consequence the damage evolution seems to be much faster than for the L orientation and damages such as small cracks and thermal shock crack networks appear already at lower power densities and higher base temperatures.
Beside the general investigation and classification of the induced thermal shock damages it is also of great importance to have a detailed look at the surface degradation due to thermal shock exposure. Figure 5 gives representative examples of the thermal shock crack propagation in the material in dependence on the microstructure.

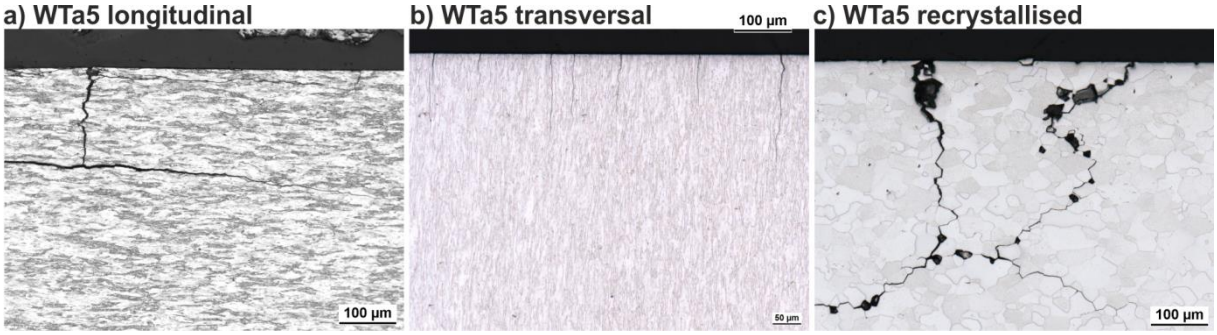

Figure 5: Light microscope images of metallographic cross section of WTa5 with (a) L, (b) T and (c) R grain orientation exposed to 100 thermal shock events at RT with an absorbed power density of 0.76 GW/m².

The crack propagation of the L (see Figure 5a) and R (Figure 5c) sample look very similar. They first propagate perpendicular to the loaded surface into the material, stop at a certain depth and start to grow parallel to the surface. These parallel cracks act as a thermal barrier and cause overheating as well as melting of the surface and pose the risk erosion of complete parts of the surface. Closer investigations show that for the L samples the cracks propagate trans- and intergranular while for the R samples the cracks predominantly grow intergranular which is a result of the poor cohesion between single grains [14]. This is also the reason for the enormous grain loss during the preparation of the cross sections and the in general much larger crack depth in the recrystallised samples. Especially the grain loss could become a major problem during long term operation. In contrast to L and R, the T samples show no cracking parallel to the loaded surface and propagate along the grain boundaries into the material. However the crack densities are much higher due to the low mechanical strength and the brittle behaviour. This causes a very dense network of leading edges on the surface which might be overheated and molten during long term operation in fusion device [15].

High pulse number tests – JUDITH 2

High pulse number tests were performed on pure tungsten with different grain structures (L, T and R) which have similar mechanical properties compared to the materials test in Section 2, Figure 2. Induced surface modifications and damages for the L samples are depicted in a damage mapping (see Figure 6) with the same colour and shape coding as for the low pulse number tests. The only difference is that the X axis shows the number of applied thermal shock pulses and not the base temperature of the samples.

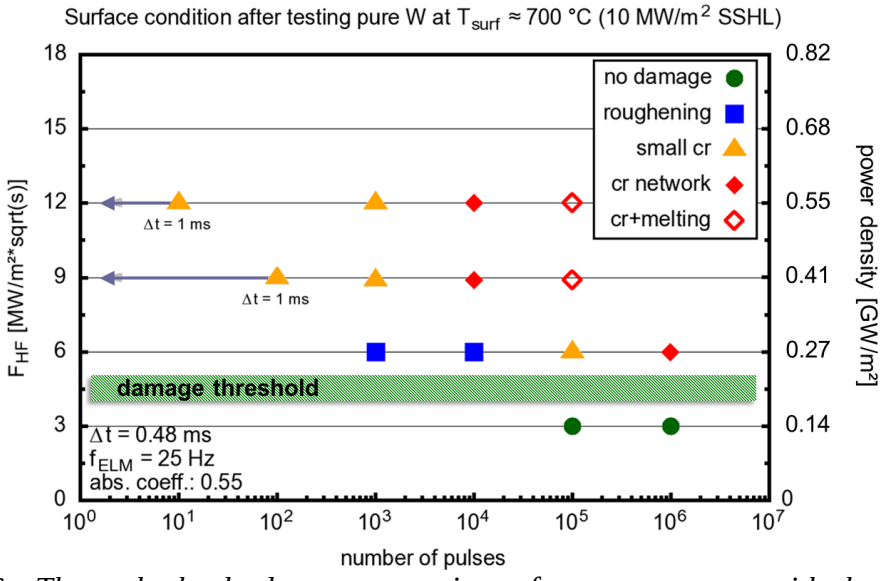

Figure 6: Thermal shock damage mapping of pure tungsten with longitudinal grain orientation at a base temperature of 700 °C [16].

In contrast to the low pulse number tests discussed before, the high pulse number tests were performed at a fixed base temperature of 700 °C and therefore the material is in a ductile regime. A promising first result is that the damage threshold stays in the same region (around 0.2 GW/m² or $F_{HF} \approx 6$ MW/m²s$^{0.5}$) as it was also found in the low pulse number tests for the L samples even after 10^6 thermal shock events. Above this threshold value fatigue effects are clearly visible. At 0.27 GW/m² the tungsten surface shows roughening due to plastic deformation up to 10^4 pulses. Further exposure induces small arbitrarily distributed cracks which results in a thermal shock crack network after 10^6 pulses. The basic damage mechanism is the same for high and low pulse number tests. During the thermal shock the materials is

subjected to thermal expansion which is restricted by the colder surrounding material and compressive stresses are induced. These stresses lead to plastic deformation if they overcome the yield strength of the material. After the thermal shock the material shrinks during the cool down phase but cannot return to its original state depending on the degree of plastic deformation and the compressive stresses are converted into tensile stresses. Depending on the base temperature, below or above DBTT, these stresses result in brittle cracks, which are formed during the first couple of pulses (see Figure 3 and Figure 4) or in fatigue cracks, respectively. Fatigue cracks are caused by the weakening of a material due by repeatedly applied loads and the accumulation of defects like dislocations. Once formed these cracks constantly grow under further loading deeper into the material [17]. This crack growth is also observed during the high pulse number tests as is can be seen in **Fehler! Verweisquelle konnte nicht gefunden werden.**.

Table 1: Crack depth evolution of tungsten with increasing number of pulses at a base temperature of 700 °C.

	10^3 pulses	**10^4 pulses**	**10^5 pulses**
0.41 GW/m²	10 ± 2 µm	53 ± 32 µm	162 ± 102 µm
0.55 GW/m²	21 ± 4 µm	63 ± 20 µm	218 ± 57 µm

Beside the already during the low pulse number tests defined damage categories a new category, cracking plus melting, was found for the high pulse number tests. A representative example for this new damage category is shown in Figure 7. Additionally to the strong plastic deformation and cracking, small droplets of molten materials are visible on the loaded surface although the surface temperature (base temperature plus temperature rise during the thermal shock of 0.55 GW/m² is ~ 1800 °C) is not high enough to melt tungsten (see Figure 7a). The explanation for this is that due to the severe plastic deformation and cracking small parts of the materials lose contact to the bulk materials. This causes a significant drop of the heat dissipation and results in overheating and melting of these structures. The lose contact of these structures also poses the risk of enhanced erosion.

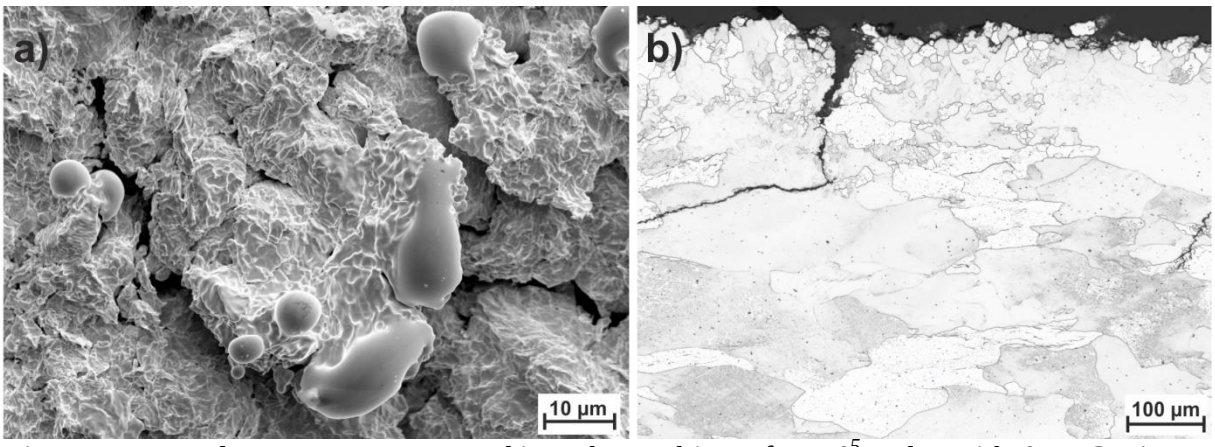

Figure 7: New damage category cracking plus melting after 10^5 pules with 0.41 GW/m² at 700 °C: (a) SEM image of the surface; (b) light microscope image of the cross section.

Metallographic cross sections of these structures (see Figure 7b) show that the fatigue cracks tend to propagate not only perpendicular but also parallel to the loaded surface which additionally causes an overheating of the surface. Furthermore, the material starts to recrystallise in a surface near region although the base temperature is below the recrystallisation temperature and only the additional temperature rise during the thermal shock heats the material above the recrystallisation temperature. Tensile test results (see Figure 2) in

combination with the low pulse number tests (see Figure 4b) show that recrystallisation has a significant influence on the mechanical properties of the materials and could increase the damage evolution significantly even if the pristine materials had much higher mechanical strength.
Analog to the low pulse number tests also the T and R microstructures were exposed to high pulse number tests. The results are shown in Figure 8. In contrast to the L material the damage threshold drops below 0.14 GW/m² ($F_{HF} \approx 3$ MW/m²s$^{0.5}$) similar to the results obtained from the low pulse number tests. Furthermore, the formation of crack starts at a lower number of pulses, i.e, small cracks are already formed after 10^4 at 0.27 GWm². Similar to the low pulse number tests the reason for this degradation of the thermal shock performance is the reduced mechanical strength of T and R compared to the L orientation. Accordingly, damage evolution for T and R is much faster than for the L orientation.

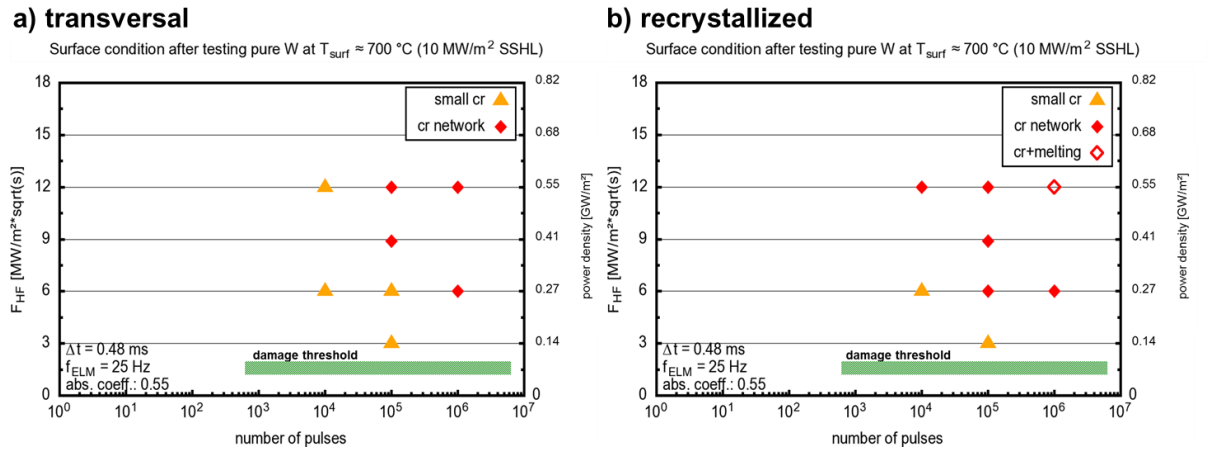

Figure 8: Thermal shock damage mapping of pure tungsten with (a) transversal and (b) recrystallised grain structure at a base temperature of 700 °C.

4 Summary & Conclusions

The obtained results show that the applied thermal shock loads induce a wide range of surface modifications and damages, which are strongly influenced by the material properties and microstructure. Low pulse number damage mappings of different tungsten products with different mechanical and microstructural properties have shown that yield/tensile strength as well as ductility have a significant influence on the damage behaviour. The transversal grain orientation, which is the preferred one for ITER, shows brittle behaviour even at elevated temperatures while recrystallised materials have a reduced mechanical strength. These changes in microstructure and materials properties lead to a significant drop of the damage threshold while the solid solution hardening with tantalum increases the mechanical strength as well as the damage threshold at the expense of a significant reduction of ductility.
High pulse number tests of one tungsten product with longitudinal and transversal grain orientation as well as in the recrystallised state support this assumption. The results clearly indicate that roughening due to plastic deformation is a precursor for fatigue crack formation. Transversal and recrystallised specimens show thermal shock damage formation even at power densities below 0.14 GW/m² ($F_{HF} \approx 3$ MW/m²s$^{0.5}$) after 10^5 pulses.
Detailed post-mortem analyses of the induced damages showed critical crack formation parallel to the loaded surface for the longitudinal and recrystallized samples, which will act as a thermal barrier and cause overheating, recrystallisation and melting of surface near regions. Enhanced erosion of surface near grains was observed for materials in the recrystallised state. This could contaminate the plasma and in the worst case cause a breakdown of the fusion reaction. Due to the reduced mechanical strength of the recrystallised materials the damage

evolution is much faster and might lead to an earlier failure of a plasma facing component. Furthermore, molten and re-solidified tungsten surfaces show very similar damage behaviour as recrystallized materials. This leads to the assumption that melting poses similar risks than recrystallization [18].
Beside the pure thermal exposure of tungsten also particle loads need to be taken into account. Especially H and He will change the mechanical and thermal properties of tungsten and hence have an influence on the thermal shock damage response. Due to H/He embrittlement critical stresses for damage/cracking formation will be lower and lead also to faster damage evolution [19, 20]. He induced bubble formation directly below the surface reduces the thermal conductivity and could lead to higher surface temperatures and W-fuzz give indications of enhanced erosion of material [21]. Moreover the impact of high neutron doses on the performance of tungsten under transient heat loads, especially for high pulse number tests and simultaneous particle exposure, are not clear yet [22].
The combination of this wide range of environmental conditions makes the evaluation of tungsten and the prediction of possible damages and life time's very difficult and complex. However, it can be assumed that recrystallisation and molten/re-solidified surface structures have detrimental influence on the lifetime of PFM and components. Therefore, further investigations of tungsten as PFM for long term operation with high accumulated neutron doses and the study of the influence of pre-damaged surfaces on the plasma performance in existing tokamaks are at the moment the important issues for future fusion reactors to be addressed.

5 Acknowledgment

This work has been carried out within the framework of the EUROfusion Consortium and has received funding from the Euratom research and training programme 2014–2018 under grant agreement No 633053. The views and opinions expressed herein do not necessarily reflect those of the European Commission. This work was done within the EUROfusion work project PFC.

6 References

[1] R.A. Pitts, S. Carpentier, F. Escourbiac, T. Hirai, V. Komarov, S. Lisgo, A.S. Kukushkin, A. Loarte, M. Merola, A. Sashala Naik, R. Mitteau, M. Sugihara, B. Bazylev, P.C. Stangeby. Journal of Nuclear Materials 428 (2013) S48-S56
[2] M. Merola, D. Loesser, A. Martin, P. Chappuis, R. Mitteau, V. Komarov, et al., Fusion Eng. Des. 85 (2010) 2312–2322
[3] A. Loarte, G. Saibene, R. Sartori, V. Riccardo, P. Andrew, J. Paley, W. Fundamenski, T. Eich, A. Herrmann, G. Pautasso, A. Kirk, G. Counsell, G. Federici, G. Strohmayer, D. Whyte, A. Leonard, R. A. Pitts, I. Landman, B. Bazylev, S. Pestchanyi. Physica Scripta, 2007 (2007) 222-228
[4] Duwe R, Kuehnlein W, Muenstermann H 1994 The new electron beam facility for materials testing in hot cells, Fusion Technology 356–358
[5] A. Schmidt, A. Bürger, K. Dominiczak, S. Keusemann, Th. Loewenhoff, J. Linke, et al., High heat flux testing of components for future fusion devices by means of the facility JUDITH 2, in: International Conference on High-Power Electron Beam Technology (EBEAM 2010), Reno (USA), 2010, ISBN 9781617823992, p. 571
[6] P. Majerus, R. Duwe, T. Hirai, W. Kühnlein, J. Linke, M. Rödig, Fusion Eng. Des. 75–79 (2005) 365–369
[7] I. Uytdenhouwen, Degradation of First Wall Materials under ITER Relevant Loading Conditions, Ph.D thesis University Gent (2010)

[8] E. Lassner and W.-D. Schubert, Tungsten: Properties, Chemistry, Technology of the Element, Alloys, and Chemical Compounds, Kluwer Academic/Plenum Publishers, New York, (1999)
[9] E. Pink and R. Eck, Refractory Metals and Their Alloys, Wiley-VCH Verlag GmbH & Co. KGaA (2006)
[10] J. P. Morniroli, Low Temperature Embrittlement of Undoped and Doped Tungsten, Elsevire, London (1989)
[11] G. L. Krask, Effect of impurities on the electronic structure of grain boundaries and intergranular cohesion in iron and tungsten, Materials Science and Engineering: A 234–236 (0), 1071–1074, (1997)
[12] W. Martienssen and H. Warlimont, Springer handbook of condensed matter and materials data, Springer Berlin, (2005)
[13] M. Wirtz, J. Linke, G. Pintsuk, L. Singheiser, I. Uytdenhouwen, Phys. Scr. T145 (2011) 014058 (4pp), doi:10.1088/0031-8949/2011/T145/014058
[14] F. J. Humphreys, M. Hatherly, Recrystallization and Related Annealing Phenomena, Pergamon 2nd edition (2003)
[15] A. Zhitlukhin, N. Klimov, I. Landman, J. Linke, A. Loarte, M. Merola, V. Podkovyrov, G. Federici, B. Bazylev, S. Pestchanyi, V. Safronov, T. Hirai, V. Maynashev, V. Levashov, A. Muzichenko, Journal of Nuclear Materials, Volumes 363–365, 15 June 2007, Pages 301-307
[16] Reprinted from Publication Fusion Engineering and Design, 87, Th. Loewenhoff, J. Linke, G. Pintsuk, C. Thomser, Tungsten and CFC degradation under combined high cycle transient and steady state heat loads, 1201 - 1205, Copyright (2012), with permission from Elsevier
[17] A. Weronski, T. Hejwowski, Thermal fatigue in Metals, Taylor & Francis, New York, (1991)
[18] Th. Loewenhoff, J. Linke, J. Matejicek, M. Rasinski, M. Vostrak, M. Wirtz, Nuclear Materials and Energy doi:10.1016/j.nme.2016.04.004 (2016) in Press
[19] M. Wirtz, S. Bardin, A. Huber, A. Kreter, J. Linke, T.W. Morgan, G. Pintsuk, M. Reinhart, G. Sergienko, I. Steudel, G. De Temmerman, B. Unterberg. Nuclear Fusion 55 (2015) 123017
[20] G. G. van Eden, T. Morgan, H. van der Meiden, J. Matejicek, T. Chraska, M. Wirtz, G. De Temmerman, Nuclear Fusion 54 (12), art. no. 123010 (2014).
[21] N. Yoshida, H. Iwakiri, K. Tokunaga, T. Baba. Journal of Nuclear Materials 337-339 (2005) 946-950
[22] G. Pintsuk, J. Compan, T. Hirai, J. Linke, M. Rödig, I. Uytdenhouwen, 2007 IEEE 22nd Symposium on Fusion Engineering, Albuquerque, NM, 2007, pp. 1-4. doi: 10.1109/FUSION.2007.4337887